Push-out tests and bond strength of rectangular CFST columns

Xiushu Qu [1,2], Zhihua Chen [*2], David A. Nethercot [3],
Leroy Gardner [3] and Marios Theofanous [4]

[1] *School of Civil and Transportation Engineering,*
Beijing University of Civil Engineering and Architecture, Beijing, 100044, PR China
[2] *School of Civil Engineering, Tianjin University, Tianjin, 300072, PR China*
[3] *Department of Civil and Environmental Engineering, South Kensington Campus*
Imperial College London, SW7 2AZ, UK
[4] *School of Civil Engineering, University of Birmingham, Edgbaston, B15 2TT, UK*

Abstract. Push-out tests have been conducted on 18 rectangular concrete-filled steel tubular (CFST) columns with the aim of studying the bond behaviour between the steel tube and the concrete infill. The obtained load-slip response and the distribution of the interface bond stress along the member length and around the cross-section for various load levels, as derived from measured axial strain gradients in the steel tube, are reported. Concrete compressive strength, interface length, cross-sectional dimensions and different interface conditions were varied to assess their effect on the ultimate bond stress. The test results indicate that lubricating the steel-concrete interface always had a significant adverse effect on the interface bond strength. Among the other variables considered, concrete compressive strength and cross-section size were found to have a pronounced effect on the bond strength of non-lubricated specimens for the range of cross-section geometries considered, which is not reflected in the European structural design code for composite structures, EN 1994-1-1 (2004). Finally, based on nonlinear regression of the test data generated in the present study, supplemented by additional data obtained from the literature, an empirical equation has been proposed for predicting the average ultimate bond strength for SHS and RHS filled with normal strength concrete.

Keywords: composite construction; concrete filled steel tubes; interface bond strength; interface condition; push-out test; slip

1. Introduction

Concrete filled steel tubular (CFST) columns exhibit numerous favourable structural properties including high strength, stiffness and ductility that make them well-suited for a range of structural applications such as high-rise buildings and bridge piers. The steel tube provides effective confinement to the concrete core, thus increasing its strength and ductility, whilst the concrete core delays and often prevents local buckling of the surrounding tube for SHS and RHS (Uy 1998), thereby also increasing the ductility of CFST members under cyclic loading (Broderick *et al.*

∗Corresponding author, Professor, E-mail: zhchen@tju.edu.cn

2005). For concrete-filled CHS the presence of concrete infill does not significantly affect the local buckling of the steel tubes (O'Shea and Bridge 2000), the failure mode of which usually assumes the form of an elephant's foot near either of the loaded ends.

The significant structural advantages of CFST over their bare steel or reinforced concrete counterparts lead to reduced section sizes and hence increased usable floor areas in the lower storeys of multi-storey buildings, reduced corrosion protection and fire proofing costs (Packer and Henderson 2003) and significant material savings (Webb and Peyton 1990). Additional financial advantages arise from the ability of the steel tubes to withstand considerable construction loads prior to hardening of the concrete and from the elimination of the need for formwork, since the steel tube acts as permanent and integral formwork, thus reducing construction times. Moreover, CFST can often be used without any fire protection (Wang and Kodur 2000), thereby further reducing construction costs.

Square, rectangular and circular hollow sections (SHS, RHS and CHS respectively) are typically employed for CFST members. However the structural response of octagonal hollow sections (Morishita *et al*. 1979b, Tomii *et al*. 1980b) and, more recently, elliptical hollow sections (Yang *et al*. 2008, Zhao and Packer 2009, Espinos *et al*. 2011, Sheehan *et al*. 2012) has also been investigated. Most of the research investigations on CFST members, a detailed account of which is given in (Shanmugam and Lakshmi 2001, Gourley *et al*. 2008), have focused on relatively thick-walled steel tubes filled with normal strength concrete, whilst thin-walled tubes filled with high-strength concrete have received less attention (O'Shea and Bridge 2000). More recently, the structural performance of stainless steel concrete-filled tubes has been studied (Young and Ellobody 2006, Lam and Gardner 2008, Uy *et al*. 2011).

Achieving composite action (i.e., transfer of shear stress between the concrete infill and the surrounding tube), either by relying on natural bond or with the aid of shear connectors, such as structural bolts (Shakir-Khalil 1993a, b, Shakir-Khalil and Hassan 1994), Hilti connectors (Shakir-Khalil 1993b), threaded bars (Shakir-Khalil and Hassan 1994), self-taping screws (Kilpatrick and Rangan 1999) and tab stiffeners (Petrus *et al*. 2011), is crucial for the satisfactory performance of CFST members particularly in the vicinity of the connections where the bond strength demand is more severe (Roeder *et al*. 1999). Moreover, the interface bond has been shown to have a marked effect on the ultimate capacity of circular CFST stub columns (O'Shea and Bridge 2000, Kilpatrick and Rangan 1999, Giakoumelis and Lam 2004), whilst its effect on the ultimate capacity of slender columns is negligible (Kilpatrick and Rangan 1999). Despite its significance, the interface bond strength between the steel and the concrete has received relatively little attention in comparison to the structural response of CFST members, as evidenced in (Shanmugam and Lakshmi 2001, Gourley *et al*. 2008). The main objective of this paper is the investigation of the main parameters affecting the interface bond strength between the steel tube and the concrete infill and the assessment of the relevant design provisions of EN 1994-1-1 (2004). To this end, an experimental study is reported in detail, following a review of past research on bond strength, which aids in the interpretation of the experimental results. Finally, a predictive empirical equation for average ultimate bond strength is proposed.

2. Past research on bond strength

The European structural design code for composite steel-concrete structures, EN 1994-1-1 (2004), specifies the design shear strength at the concrete-steel interface. If the imposed

longitudinal shear stress exceeds the specified shear strength, shear connectors must be provided to achieve composite action. In EN 1994-1-1 (2004) the design shear strength depends on whether the steel section considered is fully encased, partially encased or filled with concrete. A further distinction for concrete filled tubes is made, depending on whether the filled tube has a circular or a rectangular hollow section, to reflect the significantly enhanced bond strength displayed by concrete filled CHS over their RHS counterparts as observed by numerous researchers (Morishita *et al* .1979a, b, Shakir-Khalil 1993a, b, Roeder *et al*. 1999, Tao *et al*. 2011). This is attributed to the fact that CHS exert a uniform confining pressure on the concrete core and hence resist its slip over their entire perimeter, whereas RHS are more effective in resisting the slip of the core near the stiff corner regions with the flat parts of the sections being largely ineffective (Shakir-Khalil 1993a, b, Shakir-Khalil and Hassan 1994).

In addition to the cross-section type, numerous researchers have verified that parameters such as cross-sectional dimensions and slenderness (O'Shea and Bridge 2000, Shakir-Khalil 1993a, b, Roeder *et al*. 1999, Tao *et al*. 2011), variation in internal tube dimensions (Shakir-Khalil 1993b, Tao *et al*. 2011, Virdi and Dowling 1975), roughness of the interface (Tomii *et al*. 1980a, b, Shakir-Khalil 1993a, Roeder *et al*. 1999, Morishita *et al* .1979a, Virdi and Dowling 1975), concrete compaction (Virdi and Dowling 1975, Han and Yang 2001), age (Tao *et al*. 2011, Virdi and Dowling 1975, Aly *et al*. 2010) and shrinkage (Morishita *et al*. 1979a, b, Shakir-Khalil 1993a, Roeder *et al*. 1999, Virdi and Dowling 1975, Xu *et al*. 2009) have a significant influence on bond strength. In all cases, obtaining a satisfactory keying action between steel and concrete was shown to be a crucial factor affecting bond strength. On the contrary, the steel-concrete interface length was not found to have a direct effect on the maximum bond strength of the specimens according to (Shakir-Khalil 1993a, Virdi and Dowling 1975), though in (Tao *et al*. 2011) it was found that the bond strength increased with increasing interface length for SHS. Similarly there seems to be a lack of consensus regarding the effect of concrete grade on bond strength, with some researchers reporting that higher concrete grade leads to increased bond strengths (Xu *et al*. 2009, Xue and Cai 1996), whilst others observed the opposite trend (O'Shea and Bridge 2000, Morishita *et al* .1979a, b, Shakir-Khalil 1993a, Virdi and Dowling 1975). This is attributed to the fact that with increasing concrete strength the potential for autogenous shrinkage also increases (Virdi and Dowling 1975, Uy 2001, EN 1992-1-1 2004), particularly for CHS, where the reduction in confining pressure due to shrinkage is more pronounced. Hence, if no particular measures to mitigate shrinkage are employed (Xu *et al*. 2009), the larger autogenous shrinkage associated with increasing concrete strength may overshadow the potentially better keying action due to higher concrete strength, particularly for larger section sizes (Roeder *et al*. 1999). Hence, the effect of concrete strength on bond strength has to be treated with caution, bearing in mind the detrimental effect of shrinkage, particularly for the larger section sizes. This issue is further discussed in Sections 4 and 5.

The mechanisms contributing to bond strength have also been investigated (Shakir-Khalil 1993a, Virdi and Dowling 1975, Parsley *et al*. 2000, Qu *et al*. 2013). Generally, the interface carrying capacity can be considered to arise from a combination of three different mechanisms: chemical adhesion, microlocking and macrolocking (Tao *et al*. 2011, Virdi and Dowling 1975, Chen *et al*. 2009). According to previous research on bond in reinforced concrete, the chemical adhesion strength is very small and is influenced by many factors, such as the cement content and water-cement ratio. Due to the shape of CFST columns, the nature of bond between the concrete and steel tube may be different from that between concrete and reinforcing bars. Microlocking is caused by the roughness of the steel surface on the microscopic scale, and before the concrete core as a whole can begin to move, it is this microlocking that has to be broken (Virdi and Dowling

1975). Macrolocking, also referred to as interface friction, is due to the manufacturing tolerances associated with the internal dimensions of the tube. Its influence is largely restricted to the latter stages of the load-deflection response (Virdi and Dowling 1975).

The contribution of the three components of bond strength at the various stages of loading is shown in terms of an idealized force-slip curve in Fig. 1. Chemical adhesion and microlocking govern the initial linear part of the curve and contribute mainly to the attainment of the maximum bond stress, whereas macrolocking determines the residual bond stress that remains at the later stages of the bond stress-slip curve. Moreover, the stress-slip curve may assume three different shapes as discussed in (Tao *et al.* 2011) and shown in Fig. 2, depending on the relative contribution of macrolocking upon the loss of bond. It may display a maximum followed by a falling branch, a maximum followed initially by a falling branch, which rises again at large slips, or display no maximum at all, as was the case for all tests reported in (Virdi and Dowling 1975).

With the exception of the cross-section type and the roughness of the interface, the significance of which is acknowledged in EN 1994-1-1 (2004) by specifying that the steel section in contact with the concrete shall be unpainted and free from oil, grease and rust, no other factor affecting bond strength is accounted for either directly or indirectly in EN 1994-1-1 (2004). Moreover the basic mechanisms contributing to the ultimate bond strength are not considered. This may lead to inaccurate bond strength predictions that may be overly conservative or even unsafe. Hence further research on quantifying the effect of various factors on bond strength in accordance with the
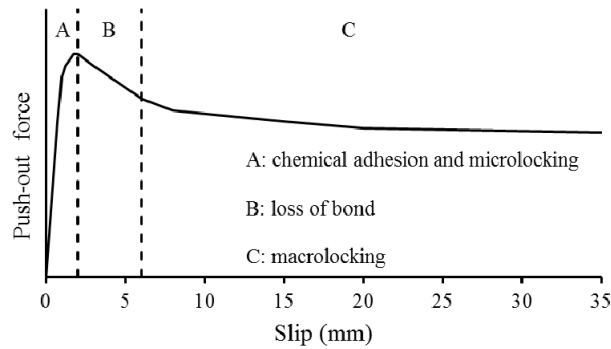

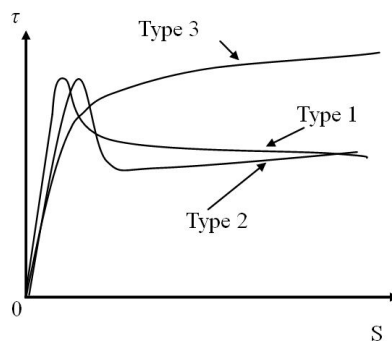Fig. 1 Idealized response of push-out specimens

Fig. 2 Three kinds of load-slip curve

experimentally observed structural response is warranted. To this end, an experimental study is reported herein, the results of which are utilized in conjunction with other available test data to quantify the effects of various parameters on the bond strength.

3. Experimental study

3.1 General

Push-out testing is the most common method used to evaluate bond capacity, with the average ultimate bond strength τ_u often being used to represent interface bond strength. This is determined from

$$\tau_u = N_u / CL_i \tag{1}$$

where N_u is the maximum load from the load-deflection curve, L_i is the length of the steel-concrete interface, and C is the perimeter of the concrete section in contact with the steel tube.

A total of 18 specimens were prepared and tested in this study. Among the various parameters mentioned previously that have been found to affect bond strength, the influence of the following four is assessed experimentally herein: (a) cross-section dimensions; (b) interface length; (c) concrete compressive strength; and (d) interface condition. Table 1 provides details of the ranges of values and treatments covered. For all specimens, designations starting with TCA refer to

Table 1 Measured geometric properties for test specimens

| Specimen reference	$D \times B \times t \times L$	L_i (mm)	Concrete strength grade	Steel grade	Interface condition
TCA-1	150×100×4.07×700	600	C30	Q235b	Lubrication
TCA-2	150×100×4.07×800	700	C40	Q235b	Lubrication
TCA-3	150×100×4.07×900	800	C50	Q235b	Lubrication
TCA-4	200×150×4.43×700	600	C50	Q235b	Lubrication
TCA-5	200×150×4.43×800	700	C30	Q235b	Lubrication
TCA-6	200×150×4.43×900	800	C40	Q235b	Lubrication
TCA-7	300×200×5.73×800	700	C40	Q345b	Lubrication
TCA-8	300×200×5.73×900	800	C50	Q345b	Lubrication
TCA-9	300×200×5.73×1000	900	C30	Q345b	Lubrication
TCB-1	150×100×4.07×700	600	C30	Q235b	No lubrication
TCB-2	150×100×4.07×800	700	C40	Q235b	No lubrication
TCB-3	150×100×4.07×900	800	C50	Q235b	No lubrication
TCB-4	200×150×4.43×700	600	C50	Q235b	No lubrication
TCB-5	200×150×4.43×800	700	C30	Q235b	No lubrication
TCB-6	200×150×4.43×900	800	C40 (2)	Q235b	No lubrication
TCB-7	300×200×5.73×800	700	C40 (2)	Q345b	No lubrication
TCB-8	300×200×5.73×900	800	C50	Q345b	No lubrication
TCB-9	300×200×5.73×1000	900	C30	Q345	No lubrication
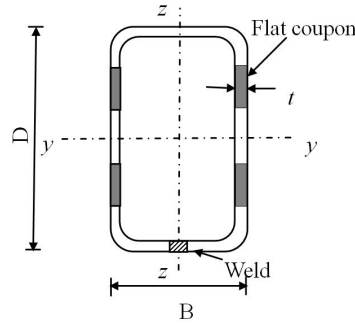
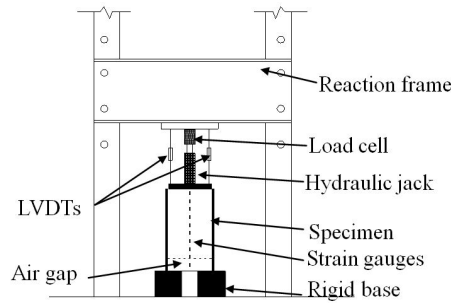Fig. 3 Section labelling convention and location of flat tensile coupons

Fig. 4 Test Setup

those which were lubricated (using butter) at the steel-concrete interface, whilst designations beginning with TCB had no lubrication. This is followed in the designation system with the specimen number from 1 to 9. The section labelling convention is shown in Fig. 3.

3.2 Preparation of specimens

The interface bond strength was measured by means of push out tests on cold-formed rectangular steel tubes filled with concrete. The ends of the steel tubes were cut and machined to the required length, ensuring that the two ends were parallel to each other and normal to the sides. Any deposits of dust or oil on the inside of the steel tubes were removed prior to casting of the concrete. In order to investigate the longitudinal strain variation along the centreline of the CFST cross-sections, a steel bar instrumented with strain gauges was embedded within the concrete core of each specimen. The concrete was cast within the steel tubes, leaving a 100 mm air gap at one end of each specimen, as shown in Fig. 2. All specimens were compacted by hand and were cured indoors for approximately 40 days prior to testing.

3.3 Material properties

3.3.1 Concrete

Three different grades of commercial concrete were used in the tests. As the first concrete grade C40 supply was insufficient for all the specimens, TCB-6 and TCB-7 used concrete from

Table 2 Key concrete properties

Concrete strength grade	Young's modulus E_c (MPa)	Compressive strength f_{cu} (MPa)
C30	26690	29
C40	29380	39
C40(2)	29120	41
C50	38070	49

Table 3 Key material properties from tensile coupons tests

Specimen	Steel grade	Young's modulus E_s (MPa)	Yield stress f_y (MPa)	Ultimate tensile strength f_u (MPa)
RHS150×100×4.07	Q235b	212300	295	496
RHS200×150×4.43	Q235b	216800	242	410
RHS300×200×5.73	Q345b	216400	336	533

another batch, as indicated in Tables 1 and 2 as C40(2). For each batch, six 100 mm concrete cubes were cast and cured in standard laboratory conditions for 28 days (GB 50152-92 1992), after which, tests to measure the Young's modulus and compressive strength of the concrete were conducted. The average measured values of the material parameters are reported in Table 2.

3.3.2 Steel

Four coupons were extracted from the wider faces of each steel tube and tested according to GB/T 228-2002 (2002) (see Fig. 3). Standard tensile coupon tests were conducted to measure the basic material properties of the tubes (i.e., Young's modulus, yield stress and ultimate tensile stress), the averages of which are given in Table 3 for each cross-section.

3.4 Experimental set-up

All specimens were tested at approximately 40 days of age. A 500 kN capacity hydraulic jack was used to conduct the push-out tests, as shown in Fig. 4. The specimens were set up in the testing machine in a vertical position with the air gap at the bottom. A layer of sand was first spread on the top surface of the specimens to ensure a uniform dispersion of stresses despite the rough concrete surface. A steel block, which had a slightly smaller cross-section than that of the concrete core, was placed on the specimen. This ensured that the load was applied only to the concrete core and allowed the concrete core to move inside the tube during testing (Tao *et al*. 2011). The load was measured by means of a load cell which was placed on the hydraulic jack. The movement of the concrete core with respect to the steel tube at the top end was measured using two linearly varying displacement transducers (LVDTs) located at the two sides of the specimen. The deflection of the concrete core was then taken as the average of the two transducer readings. In order to study the strain distribution in the steel hollow section and at the centre of the concrete core, a series of strain gauges was affixed to the steel tubes and to a central steel bar. The spacing between two adjacent strain gauges was 100 mm. Since the strain may vary significantly near to the loaded end, three strain gauges, placed 50 mm from the loaded end, were added to the steel tube and the steel bar to capture the expected sharp variations in strain. The locations of the

strain gauges are shown, for specimen TCA-1, in Fig. 5.

During testing, the load was applied at the top of the specimen to the concrete core and was resisted at the base by the steel section alone. Initially, load was increased at the rate of 10 kN per minute and the deflections were recorded every 2 kN. Once the specimen started to show a marked change in the slip between the steel tube and concrete core, as indicated by the LVDTs, the recordings were taken every 2 mm of movement of the concrete core. The load had an available travel of 45 mm.

3.5 Experimental results

For most specimens, the initial load-slip response was approximately linear. At higher loads, the rate of slip increased until the interface carrying capacity was reached, following which the load began to decline. Eventually, the load dropped to a steady value and the bond between the steel and the concrete was destroyed. Following completion of the tests, the state of the concrete contact surface could be examined – see Figs. 6(a)-(b) showing typical lubricated and non-lubricated specimens, respectively. For both cases, evidence of concrete failure was seen predominantly in the corner regions and on some of the flat surfaces, clearly indicating that the bond between the steel and the concrete was broken.

The push-out load-slip curves for each specimen are shown in Fig. 7. All the curves can be classified into three types, as defined in Fig. 2. Type 1 has an initial linear portion, followed by a
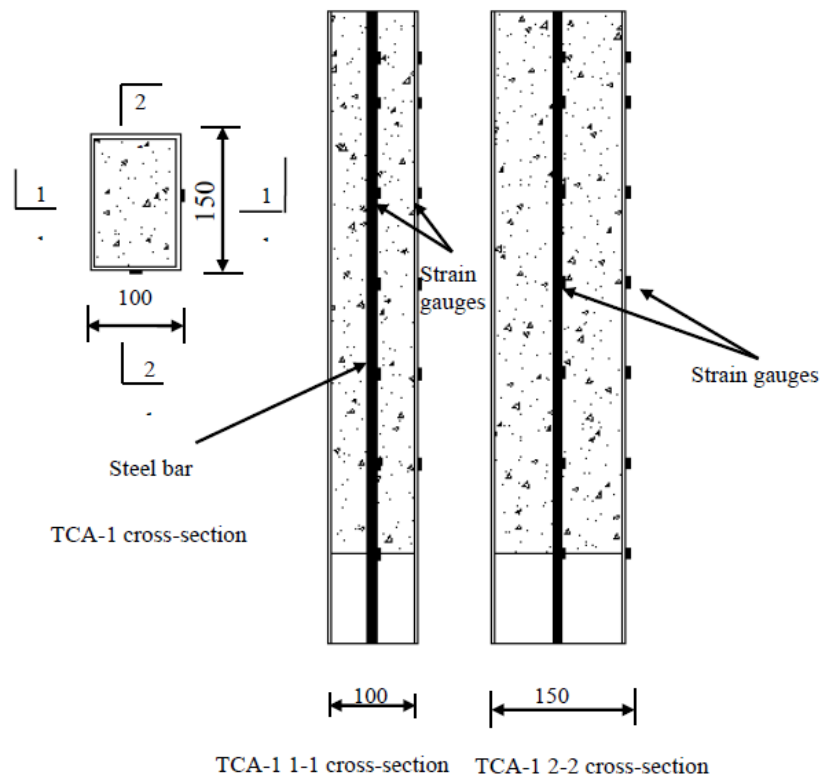

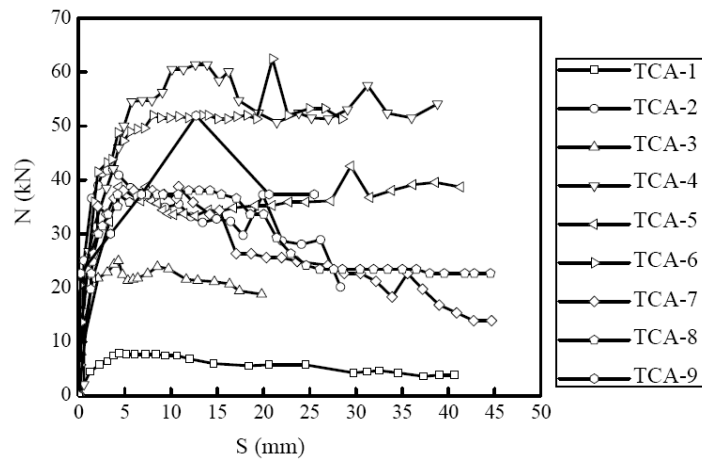Fig. 5 Specimens details: TCA-1 (dimensions in mm)

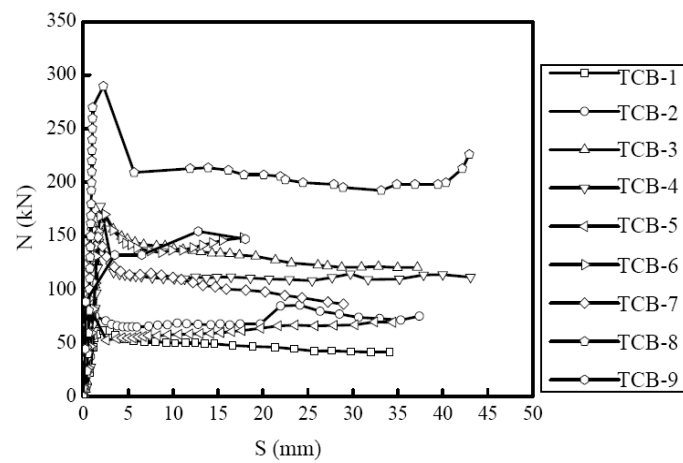(a) TCA-8 (lubricated)

(b) TCB-8 (no lubrication)

Fig. 6 View of specimens after testing

(a) Group TCA (lubricated)

(b) Group TCB (no lubrication)

Fig. 7 Push-out load-slip curves for each specimen

transitional portion. After reaching the peak strength, a rapidly declining region appears before a relatively stable residual strength is achieved. Type 2 exhibits similar features to Type 1 except for the existence of the second ascending portion after the peak bond strength. The curve tends to flatten after this second peak bond strength is achieved. Type 3 is characterized by the lack of any falling branch. Twelve specimens demonstrated the Type 1 behaviour, five exhibited Type 2 behaviour and one specimen showed the Type 3 response. It should be noted that for three of the specimens (TCA-5, TCA-6 and TCB-2) that featured Type 2 behaviour, their second peak bond strengths were marginally higher than their first peak bond strengths.

In the lubricated specimens, slip occurred at lower load levels than in the non-lubricated ones, as depicted in Fig. 7, and once slip occurred, it developed at an increasing rate. It seems that the curve type has no direct relation to the studied influence factors and is mainly dependant on the relative contribution of friction (i.e., microlocking) and macrolocking upon the initiation of slip (Tao *et al*. 2011). The main conclusion that may be drawn from all the test results is that the interface carrying capacity and load-slip curve are rather sensitive to the interface conditions.

4. Analysis of test results

It should be noted that the effect of steel grade on bond strength was not investigated herein, despite the fact that due to limited availability of the required cross-sections, two different steel grades have been utilised in this investigation. However, given the low stress level of the average ultimate bond and the fact that no permanent deformations of the steel tubes were observed upon the completion of the tests, it can be concluded that the steel tubes remained elastic throughout the tests and hence their steel grade is not expected to have any effect on the attained bond strength.

4.1 Interface bond strength

In accordance with previous practice, the average bond stress is adopted to represent interface bond strength. According to Eq. (1), the average ultimate bond strength τ_u in this study can be given by

$$\tau_u = \frac{N_u}{(2(B-2t)+2(D-2t))L_i} \tag{2}$$

where N_u is the ultimate interface bearing capacity, B is the width of the steel section, D is the depth of the steel section, t is the thickness of the steel tube, and L_i is the length of the steel-concrete interface.

Using the test results, the corresponding values of τ_u were calculated for each specimen and are shown in Table 4. The average value of τ_u for all specimens in the normal condition (Group TCA) was 0.29 MPa, while for the lubricated specimens (Group TCB), this value was 0.08 MPa, thus verifying the adverse effect of the lubrication of the interface on the bond strength.

4.2 Bond stress distribution

To further understand the bond mechanisms, it is necessary to check the bond stress distribution along the length of the tubes. The bond stresses can be obtained directly from the axial strain gradients in the steel tube, which are related by statics to the interface bond stress

Table 4 Summary of test results

Specimen reference	S_u (mm)	N_u (kN)	τ_u (MPa)	Specimen reference	S_u (mm)	$\underline{N_u}$ (kN)	τ_u (MPa)
TCA-1	4.39	7.89	0.028	TCB-1	2.26	61.8	0.220
TCA-2	3.12	41.5	0.127	TCB-2	1.33	75.1	0.229
TCA-3	4.32	25.0	0.067	TCB-3	1.93	171	0.457
TCA-4	13.9	61.4	0.154	TCB-4	1.94	178	0.445
TCA-5	4.35	38.7	0.083	TCB-5	0.952	79.8	0.172
TCA-6	8.05	52.0	0.098	TCB-6	2.42	170	0.320
TCA-7	10.8	38.8	0.058	TCB-7	1.01	156	0.234
TCA-8	14.2	38.1	0.050	TCB-8	2.24	290	0.379
TCA-9	12.7	52.0	0.061	TCB-9	3.52	132	0.154

distribution (Roeder *et al*. 1999). If N_x is the axial load in the steel tube at location x, then the bond stress, $\tau(x)$, is given by

$$\tau(x) = \frac{dN_u}{[2(B-2t)+2(D-2t)]dx} \tag{3}$$

where $dN_x = A_s E_s d\varepsilon_x$ and $d\varepsilon_x$ is the axial strain of the steel tube at location x. The strain ε_x is measured by the strain gauges, which are affixed to the steel surface. Given that the spacing between two adjacent strain gauges was 100 mm, the measured value of each strain gauge at location x can be assumed to be the strain value of the location from $(x-50)$ mm to $(x+50)$ mm. Other symbols are as previously defined.

To demonstrate how the bond stress developed under increasing load, the results from specimens TCA-1 and TCB-1 were examined in more detail, and were representative of the other samples within their respective groups. The axial strains in the narrow and wide faces of the steel
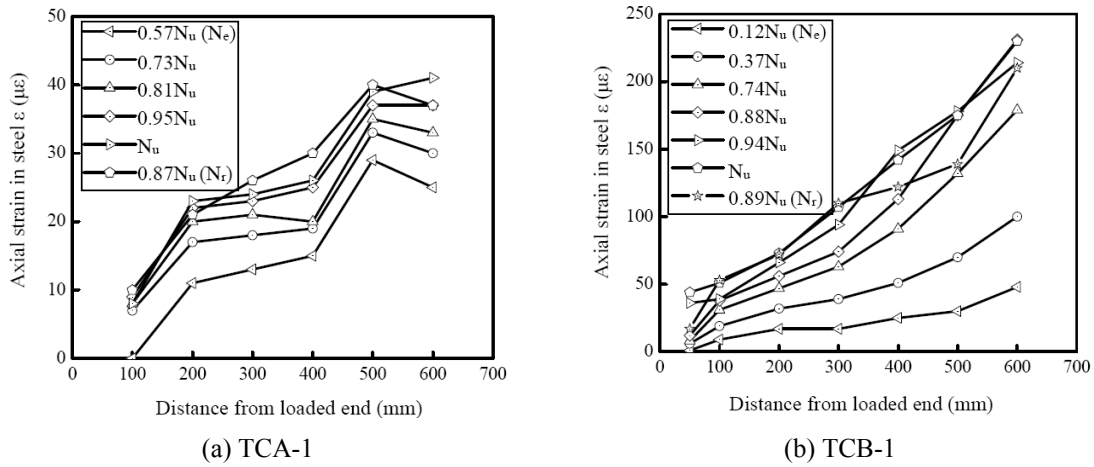

(a) TCA-1

(b) TCB-1

Fig. 8 Axial strains in narrow face of steel tubes along specimen lengths at different load levels

tube along the specimen lengths are shown in Figs. 8 and 9, respectively, at various load levels. Generally, the axial strains increased with increasing distance from the loaded end, especially at the top of the specimen, indicating a rapid development of local bond stress in this area. At the initial stage, significant contact pressure between the steel and concrete due to the Poisson effect can further increase the bond stress capacity by enhancing the friction between the two materials.

The axial strain in the concrete core can be taken as the strain in the steel bar. Figs. 10(a)-(b) show the variation in axial strains in the steel bar along the length of specimens TCA-1 and TCB-1, respectively. The strain readings at a distance of 50 mm from the loaded end of specimen TCA-1 are not displayed in Fig. 10(a) as they are considered inaccurate, perhaps due to poor affixing of the strain gauges to the steel tube at this location.

With the aid of Eq. (3), Figs. 11 and 12 have been plotted, which display the bond stress distribution along the length of specimens TCA-1 and TCB-1, respectively, at various load levels.

(a) TCA-1   (b) TCB-1
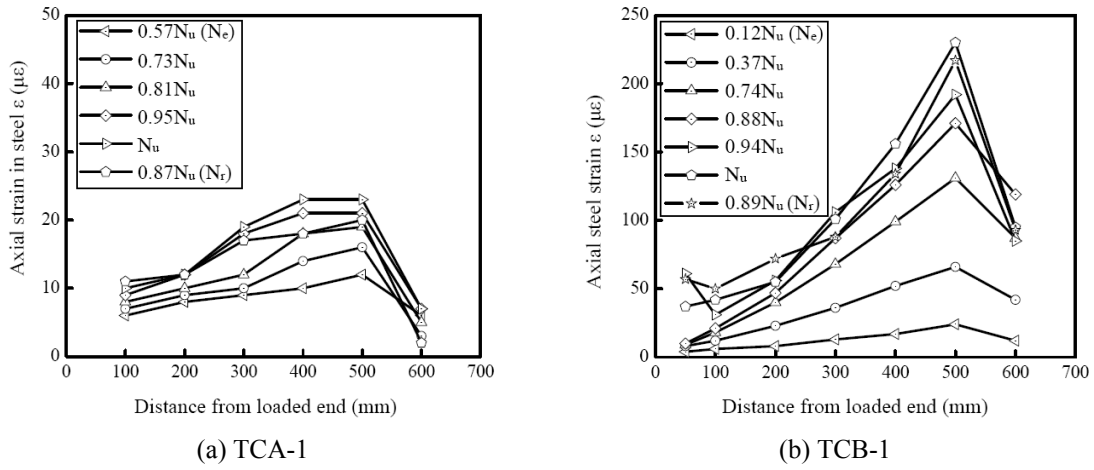
Fig. 9 Axial strains in wide face of steel tubes along specimen lengths at different load levels
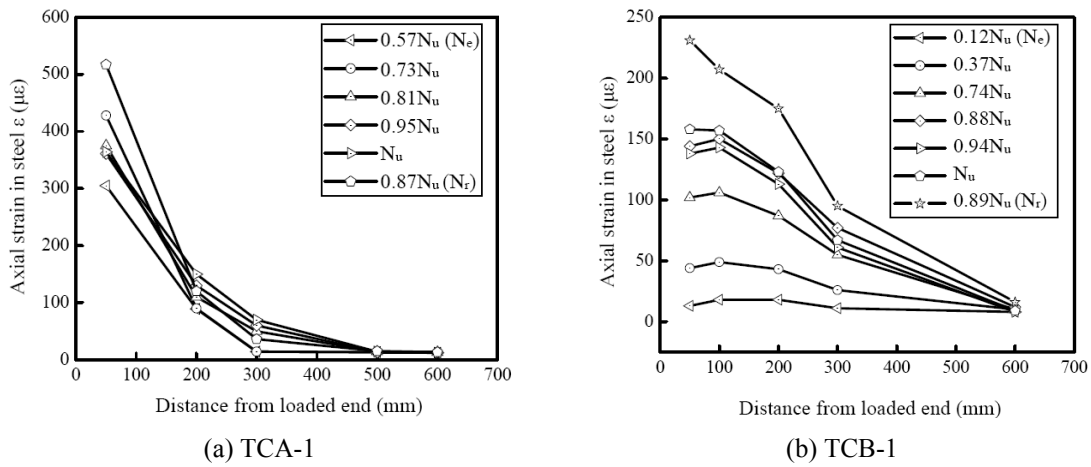

(a) TCA-1   (b) TCB-1

Fig. 10 Axial strains in central steel bar along specimen length

(a) TCA-1

(b) TCB-1

Fig. 11 Bond stress distribution in the narrow face of the steel tubes along specimen lengths at different load level
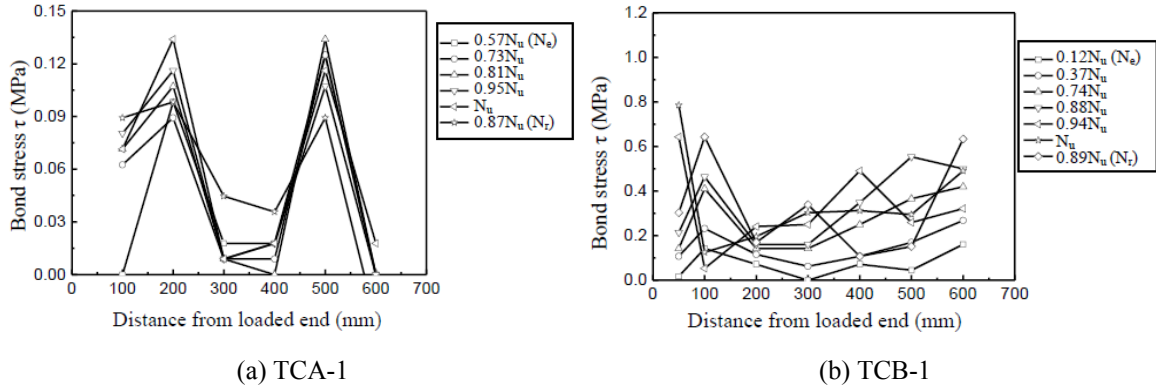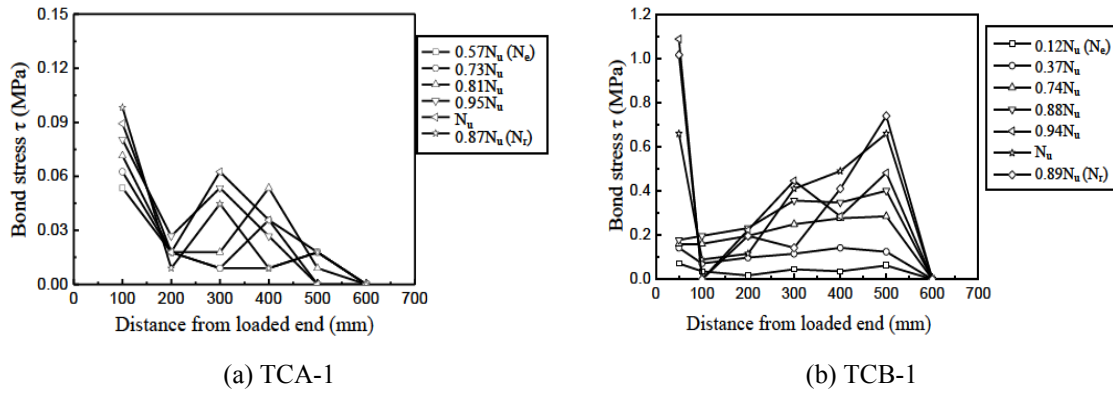

(a) TCA-1

(b) TCB-1

Fig. 12 Bond stress distribution in the wide faces of the steel tubes along specimen length at different load levels

The distribution is not uniform, but the value of local bond stress increases with increased load until the ultimate load is reached, after which the local bond stress is redistributed. Higher bond stresses are generally observed near the specimen ends. The general variation in the stress distribution may be attributed to irregularities in the steel sections. Moreover, a non-uniform distribution of bond stresses is expected around the cross-section with the local bond stresses assuming their maximum value in the vicinity of the corner regions. No attempt to quantify the non-uniformity of stresses around the cross-section was made, since this paper focuses mainly on quantifying the effect of various parameters on the average ultimate bond stress; hence local bond stresses, the distribution of which is expected to be complex and extremely sensitive to local irregularities of the interface are not considered.

4.3 Influence of different parameters

The influence of various parameters on the average ultimate interface bond strength is studied in this section.

4.3.1 Effect of interface condition

The adverse effect of lubrication on the bond stress can be clearly seen in the summary of experimental results presented in Table 4. The ultimate bond strengths achieved for the lubricated TCA series of specimens, which are attributed largely to microlocking, are between about 10%-50% of those achieved in the TCB series, where no lubrication was present, as shown in Table 5 and Fig. 13 .Comparable values from the literature (Virdi and Dowling 1975, Qu *et al.* 2013, Chen *et al.* 2009) of 10%-20% for square CFST specimens and 32%-75% for circular CFST specimens, respectively, have been reported. Based on the composition and variation in the interface bearing capacity, it can be assumed that the ultimate average bond stress for the lubricated specimens is derived, for the most part, from microlocking.

Table 5 Ratio of microlocking to average ultimate bond strength

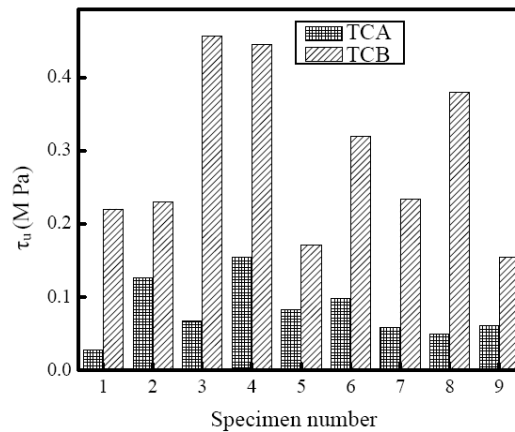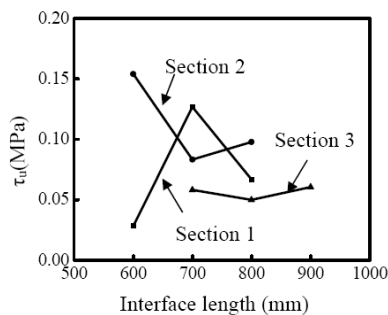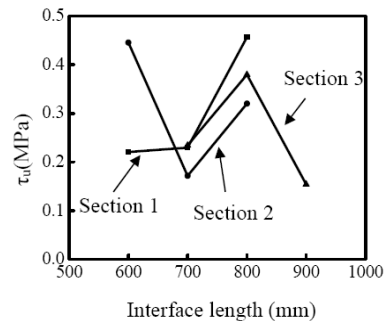| Specimen reference	TC-1	TC-2	TC-3	TC-4	TC-5	TC-6	TC-7	TC-8	TC-9
τ_{uA} / τ_{uB}	12.8%	55.2%	14.6%	34.6%	48.5%	30.6%	24.8%	13.1%	39.2%

Fig. 13 Comparison between τ_u for TCA and TCB

(a) Group TCA   (b) Group TCB

Fig. 14 Variation of average ultimate bond strength with interface length

4.3.2 Effect of interface length

Four different interface lengths – 600 mm, 700 mm, 800 mm and 900 mm – were examined in the testing programme. The variation of average ultimate bond strength with interface length is shown in Fig. 14, where in accordance with previous studies (Shakir-Khalil 1993a, Virdi and Dowling 1975), no clear correlation between interface length and average ultimate bond strength can be observed. Hence, it is confirmed that the interface length has no significant influence on the bond strength, apart from the potentially increased contribution from Macrolocking due to the greater dimensional variation associated with increasing tube length (Tao *et al*. 2011).

4.3.3 Effect of concrete strength

The variation of bond strength with concrete compressive strength is shown in Figs. 15(a) and (b) for the TCA and TCB groups, respectively. From Fig. 15(b) it may be seen that concrete compressive strength has a distinct effect on the average interface bond strength for the specimens in the normal condition; the interface bond strength generally increases with concrete strength. For the lubricated specimens, the response of which is depicted in Fig. 15(a), it may be concluded that the concrete compressive strength does not have any appreciable influence on bond strength. On the other hand, in Fig. 15(b) it may be seen that the three specimens within each group of concrete compressive strength (C30, C40 and C50) in the TCB series exhibit a similar trend, with increasing concrete strength corresponding to increased bond strength. However the effect of concrete strength has to be examined in conjunction with the effect of cross-section size since, as mentioned earlier, the higher shrinkage associated with higher concrete grades has a more adverse effect with increasing section size.

4.3.4 Effect of cross-section geometry

Three different RHS geometries were employed in the experimental part of this investigation, each having different cross-section slenderness (i.e., the maximum flat width-to-thickness ratio D/t) ranging from 35 to 50 and different outer dimensions. It has been previously observed that the bond strength decreases with increasing slenderness for CHS (Roeder *et al*. 1999, Tao *et al*. 2011). However, due to the non-uniform distribution of bond strength, the flat parts of the tubes are far less effective than the corners in resisting push-out forces compared to the much stiffer corner regions. Hence, increasing the cross-section slenderness is not expected to have a significant effect

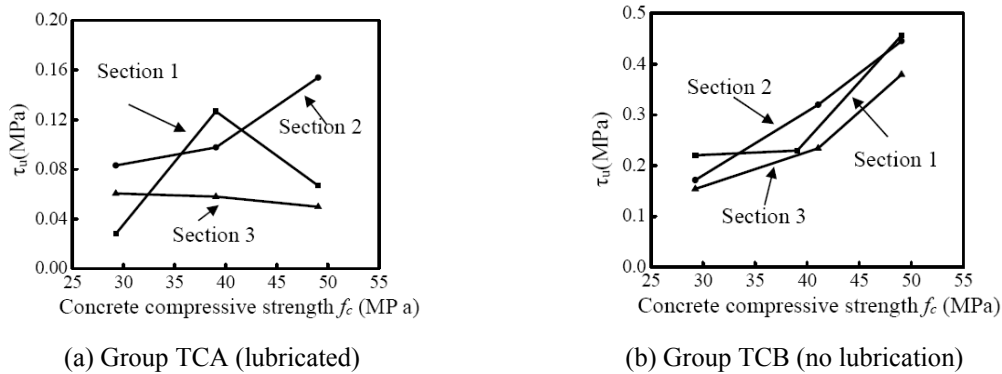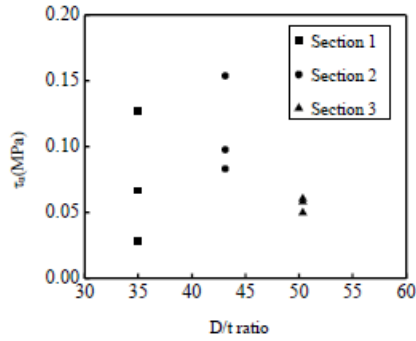(a) Group TCA (lubricated)   (b) Group TCB (no lubrication)
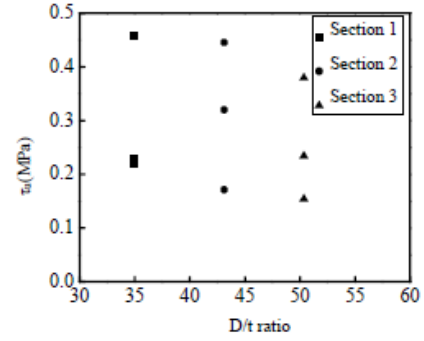
Fig. 15 Variation of average ultimate bond strength with concrete compressive strength
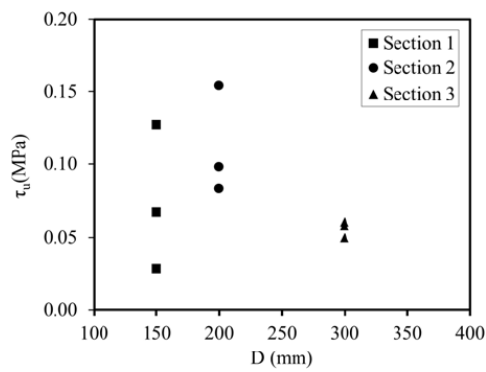
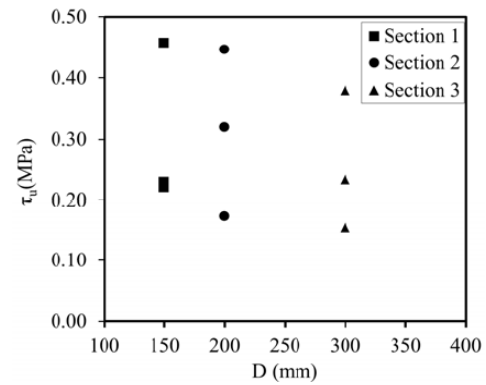(a) Group TCA (lubricated)   (b) Group TCB (no lubrication)

Fig. 16 Variation of average ultimate bond strength with D/t ratio

(a) Group TCA (lubricated)   (b) Group TCB (no lubrication)

Fig. 17 Variation of average ultimate bond strength with larger outer cross-section dimension
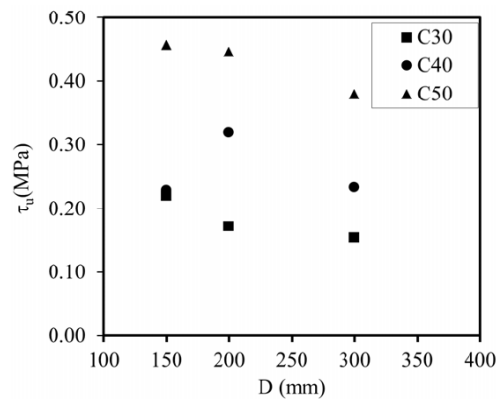

Fig. 18 Variation of average ultimate bond strength with larger outer dimension for different concrete strengths
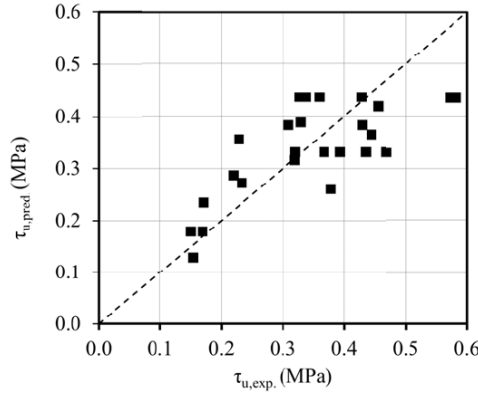
Fig. 19 Comparison of empirical equation with test data

on the average ultimate bond strength. This is confirmed by Fig. 16, where it is shown that the bond strength is insensitive to cross-section slenderness. However, increasing the cross-section size can be seen to lead to a reduction in average ultimate bond strength in Fig. 17, mainly for the non-lubricated specimens (Fig. 17(b)). This is due to the effect of shrinkage being more pronounced for larger section sizes. Hence both concrete strength and cross-section size have to be accounted for when determining the bond strength, as discussed in Section 5. The effect of both of these parameters is clearly shown in Fig. 18 for the non-lubricated specimens.

5. Empirical equation for the prediction of bond strength

Previous researchers have attempted to develop an empirical equation for predicting bond strength on the basis of experimental results. Xu *et al.* (2009) proposed an empirical equation based on an experimental investigation on the effect of prestress due to the use of expansive cement and concrete compressive strength, which is similar to an existing equation proposed by Cai (2003). In both cases the bond strength increases with increasing concrete strength, without any explicit allowance for other factors known to affect the bond strength such as the size of the filled tube. On the contrary, Roeder *et al.* (1999) proposed an empirical equation which only accounts for cross-section geometry, since in their studies they concluded that the tube overall dimensions and the D/t ratio have a pronounced effect on bond strength, whilst the concrete strength does not, owing to the increased shrinkage associated with increased concrete strength. Clearly, both factors have a significant effect on bond strength, at least for small to medium-sized tubes, whilst for larger tubes, it may be assumed that the effect of concrete strength is less pronounced as shown in (Roeder *et al.* 1999).

The aforementioned empirical equations have been derived for concrete-filled CHS. Differences in section shape affect the interface bond stress distribution along the cross-section perimeter, with rectangular CFST specimens having lower bond strengths than circular ones. Therefore, these equations are not suitable for direct use with the experimental results presented in this paper. Hence, an empirical equation is derived herein for concrete-filled RHS, which accounts for both concrete strength and cross-section size. To this end, a linear regression analysis based on a total of 28 test results, comprising the test data on non-lubricated specimens reported herein as

well as relevant test data reported in (Shakir-Khalil 1993a, Tao *et al.* 2011, Chen *et al.* 2009), has been performed. It was assumed that the bond strength decreases with increasing outer dimensions and increases in proportion to the square root of the concrete strength; a similar trend was found in (Cai 2003) and (Xu 2009) where the concrete strength was raised to the power of 0.4 and 0.44 respectively. Following a regression analysis, Eq. (4) is proposed for predicting average ultimate bond strengths for square and rectangular CFST columns.

$$\tau_u = 0.082\sqrt{f_{cu}} - 0.00105D \qquad (4)$$

where f_{cu} is the compressive cube strength of concrete in N/mm^2 and D is the larger outer dimension of the tube considered in mm.

A comparison between the test data and Eq. (4) is shown in Fig. 19. The predicted to experimental bond strength ratio has a mean value of 0.98 and a coefficient of variation of 0.28. The relatively large coefficient of variation can be largely attributed to the high sensitivity of the bond strength to factors such as the internal surface roughness and variations in internal tube dimensions (i.e., microlocking and macrolocking) which are difficult to quantify, as evidenced by the large scatter exhibited in tests of nominally identical specimens (Shakir-Khalil 1993a). Finally, it should be noted that the scope of the empirical equation is limited to non-lubricated specimens with normal concrete strength (i.e., concrete strength less than 55 MPa) and to SHS and RHS with an external depth of up to 400 mm, as dictated by the range of the relevant parameters of the utilized test data (Shakir-Khalil 1993a, Tao *et al.* 2011, Chen *et al.* 2009). It is expected that the empirical equation will not be accurate for high strength concrete due to difference shrinkage characteristics.

6. Conclusions

An experimental investigation to quantify and assess the effect of various parameters on the bond strength between rectangular steel tubes and concrete infill has been reported. A total of 18 CFST specimens with different interface conditions, concrete strength, cross-section dimensions and interface length were tested. The lubrication of the steel-concrete interface was shown to induce a significant reduction in the bond strength, with lubricated specimens (TCA) displaying a bond strength ranging from 13% to 55% of the respective bond strength of identical specimens with no lubrication (TCB). Among the other parameters investigated, concrete compressive strength and tube section size were shown to have the most important influence on bond strength. Finally, using regression analysis, an empirical equation has been proposed to predict the average ultimate bond strength for rectangular CFST columns, within a range of concrete strengths and cross-section sizes typically encountered in structural applications.

Acknowledgments

References

Aly, T., Elchalakani, M., Thayalan, P. and Patnaikuni, I. (2010), "Incremental collapse threshold for push-out resistance of circular concrete filled steel tubular columns", *J. Construct. Steel Res.*, **66**(1), 11-18.

Broderick, B.M., Goggins, J.M. and Elghazouli, A.Y. (2005), "Cyclic performance of steel and composite bracing members", *J. Construct. Steel Res.*, **61**(4), 493-514.

Cai, S.H. (2003), *Modern Steel Tube Confined Concrete Structures*, China Communication Press, Beijing, China.

Chen, Z.H., Qu, X.S., Wang, X.D., Sun, R.R. and Li, L.M. (2009), "Experimental Study on the Interface bearing capacity on concrete-filled square steel tube", *J. Harbin Inst. Technol.*, **41**(Sup 2), 27-32. [In Chinese]

EN 1992-1-1 (2004), Design of concrete structures - Part 1-1: General rules and rules for buildings, CEN.

EN 1994-1-1 (2004), Eurocode 4: Design of composite steel andconcrete structures – Part 1.1: General rules and rules for buildings, CEN.

Espinos, A., Gardner, L., Romero, M.L. and Hospitaler, A. (2011), "Fire behaviour of concrete filled elliptical steel columns", *Thin-Wall. Struct.*, **49**(2), 239-255.

GB50152-92 (1992), Standard methods for testing of concrete structures; Chinese Standard, Beijing, China.

GB/T 228-2002 (2002), Metallic materials – Tensile testing at ambient temperature; Chinese Standard, Beijing, China.

Giakoumelis, G. and Lam, D. (2004), "Axial capacity of concrete-filled tube columns", *J. Construct. Steel Res.*, **60**(7), 1049-1068.

Gourley, B.C., Tort, C., Denavit, M.D., Schiller, P.H. and Hajjar, J.F. (2008), "A synopsis of studies of the monotonic and cyclic behavior of concrete-filled steel tube members, connections and frames", Report No. NSEL-008; Newmark Structural Engineering Laboratory, Department of Civil and Environmental Engineering, University of Illinois at Urbana-Champaign, Champaign, IL, USA.

Han, L.-H. and Yang, Y.-F. (2001), "Influence of concrete compaction on the behavior of concrete filled steel tubes with rectangular secrions", *Adv. Struct. Eng.*, **4**(2), 93-100.

Kilpatrick, A.E. and Rangan, B.V. (1999), "Influence of interfacial shear transfer on behavior of concrete-filled steel tubular columns", *Struct. J.*, ACI, **96**(4), 642-648.

Lam, D. and Gardner, L. (2008), "Structural design of stainless steel concrete filled columns", *J. Construct. Steel Res.*, **64** (11), 1275-1282.

Morishita, Y., Tomii, M. and Yoshimura, K. (1979a), "Experimental studies on bond strength in concrete filled circular steel tubular columns subjected to axial loads", *Trans. Japan Concrete Inst.*, **1**, 351-358.

Morishita, Y., Tomii, M. and Yoshimura, K. (1979b), "Experimental studies on bond strength in concrete filled square and octagonal steel tubular columns subjected to axial loads", *Trans. Japan Concrete Inst.*, **1**, 359-366.

O'Shea, M.D. and Bridge, R.Q. (2000), "Design of circular concrete filled thin-walled steel tubes", *J. Struct. Eng.*, ASCE, **126**(11), 1295-1303.

Packer, J.A. and Henderson, J.E. (2003), *Hollow Structural Section Connections and Trusses – A Design Guide*, Canadian Institute of Steel Construction (CISC), Toronto, Canada.

Parsley, M.A., Yura, J.A. and Jirsa, J.O. (2000), Push-out behavior of rectangular concrete-filled steel tubes, Composite and Hybrid Systems; ACI SP-196, ACI, Farmington Hills, MI, USA.

Petrus, C., Hamid, H.A., Ibrahim, A. and Nyuin, J.D. (2011), "Bond strength in concrete filled built-up steel tube columns with tab stiffeners", *Can. J. Civil Eng.*, **38**(6), 627-637.

Qu, X., Chen Z., Nethercot, D.A., Gardner, L. and Theofanous, M. (2013), "Load-reversed push-out tests on

rectangular CFST columns", *J. Construct. Steel Res*., **81**, 35-43.

Roeder, C.W., Cameron, B. and Brown, C.B. (1999), "Composite action in concrete filled tubes", *J. Struct. Eng*., *ASCE*, **125**(5), 477-484.

Shakir-Khalil, H. (1993a), "Push-out strength of concrete-filled steel hollow sections", *Struct. Eng*., **71**(13), 230-233.

Shakir-Khalil, H. (1993b), "Resistance of concrete-filled steel tubes to push out forces", *Struct. Eng*., **71**(13), 234-243.

Shakir-Khalil, H. and Hassan, N.K.A. (1994), "Push-out resistance of concrete-filled tubes", *Proceedings of the 6th International Symposium on Tubular Structures*, Melbourne, Australia, December, pp. 285-291.

Shanmugam, N.E. and Lakshmi, B. (2001), "State of the art report on steel-concrete composite columns", *J. Construct. Steel Res*., **57**(10), 1041-1080.

Sheehan, T., Dai, X.H., Chan, T.M. and Lam, D. (2012), "Structural response of concrete-filled elliptical steel hollow sections under eccentric compression", *Eng. Struct*., **45**, 314-323.

Tao, Z., Han, L.H., Uy, B. and Chen, X. (2011), "Post-fire bond between the steel tube and concrete in concrete-filled steel tubular columns", *J. Construct. Steel Res*., **67**(3), 484-496.

Tomii, M., Yoshimura, K. and Morishita, Y. (1980a), "A method of improving bond strength in between steel tube and concrete core cast in circular steel tubular columns", *Trans. Japan Concrete Inst*., **2**, 319-326.

Tomii, M., Yoshimura, K. and Morishita, Y. (1980b), "A method of improving bond strength in between steel tube and concrete core cast in square and octagonal steel tubular columns", *Trans. Japan Concrete Inst*., **2**, 327-334.

Uy, B. (1998), "Local and post-local buckling of concrete filled steel welded box columns", *J. Construct. Steel Res*., **47**(1-2), 47-72.

Uy, B. (2001), "Static long-term effects in short concrete filled steel box columns under sustained loading", *ACI Struct. J*., **98**(1), 96-104.

Uy, B., Tao, Z. and Han, L.-H. (2011), "Behaviour of short and slender concrete-filled stainless steel tubular columns", *J. Construct. Steel Res*., **67**(3), 360-378.

Virdi, K.S. and Dowling, P.J. (1975), "Bond strength in concrete filled circular steel tubes", Composite columns, CESLIC Report; CC11, Engineering Structures Laboratories, Civil Engineering Department, Imperial College London, London, UK.

Wang, Y. and Kodur, V. (2000), "Research toward the use of unprotected steel structures", *J. Struct. Eng*., *ASCE*, **126**(12), 1442-1450.

Webb, J. and Peyton, J.J. (1990), "Composite concrete filled steel tube columns", *Proceedings of the 2nd National Structures Conference*, The Institution of Engineers Australian, Adelaide, Australia, pp. 181-185.

Xu, C., Chengkui, H., Decheng, J. and Yuancheng, S. (2009), "Push-out test of pre-stressing concrete filled circular steel tube columns by means of expansive cement", *Construct. Build. Mater*., **23**(1), 491-497.

Xue, L.H. and Cai, S.H. (1996), "Bond strength at the interface of concrete-filled steel tubular columns: part I", *Build. Sci*., **12**(3), 22-28. [In Chinese]

Yang, H., Lam, D. and Gardner, L. (2008), "Testing and analysis of concrete-filled elliptical hollow sections", *Eng. Struct*., **30**(12), 3771-3781.

Young, B. and Ellobody, E. (2006), "Experimental investigation of concrete-filled cold-formed high strength stainless steel tube columns", *J. Construct. Steel Res*., **62**(5), 484-492.

Zhao, X.L. and Packer, J.A. (2009), "Tests and design of concrete-filled elliptical hollow section stub columns", *Thin-Wall. Struct*., **47**(6-7), 617-628.

CC

Symbols

B = Width of the rectangular steel tube;

CFST = Concrete-filled steel tube;

CHS = Circular hollow section;

D = Depth of the rectangular steel tube;

E_c = Young's modulus of concrete;

E_s = Young's modulus of rectangular steel tube;

f_{cu} = Compressive cube strength of concrete;

f_y = Yield strength of steel;

f_u = Ultimate strength of steel;

L = Length of the rectangular steel tube;

L_i = Length of the steel-concrete interface;

N_u = Ultimate interface bearing capacity;

N_r = Push-out load at the end of rapidly declining portion;

$N(x)$ = Axial load in the steel tube at location x;

RHS = Rectangular hollow section;

S = Slip;

S_u = Slip corresponding to ultimate interface bearing capacity N_u;

SHS = Square hollow section;

T = Wall thickness of the steel tube;

τ = Interface bond strength;

τ_u = Average ultimate bond strength

$\tau(x)$ = Bond stress at location x;